Water-Induced Separation of Polymers from High Nanoparticle-Content Nanocomposite Films

*Baekmin Q. Kim, Máté Füredi, R. Bharath Venkatesh, Stefan Guldin, and Daeyeon Lee**

B. Q. Kim, R. B. Venkatesh, D. Lee
Department of Chemical and Biomolecular Engineering, University of Pennsylvania, Philadelphia, Pennsylvania 19104, United States
E-mail: daeyeon@seas.upenn.edu

M. Füredi, S. Guldin
Department of Chemical Engineering, University College London, London WC1E 7JE, United Kingdom

Keywords: polymer nanocomposites, composite recycling, capillary condensation, porous materials

Polymer nanocomposites with high loadings of nanoparticles (NPs) exhibit exceptional mechanical and transport properties. Separation of polymers and NPs from such nanocomposites is a critical step in enabling recycling of these components and reducing the potential environmental hazards that could be caused by the accumulation of nanocomposite wastes in landfills. However, the separation typically requires use of organic solvents or energy-intensive processes. Using polydimethylsiloxane (PDMS)-infiltrated SiO_2 NP films, we demonstrate that the polymers can be separated from the SiO_2 NP packings when these nanocomposites are exposed to high humidity and water. Our findings indicate that the charge state of the NPs plays a significant role in the propensity of water to undergo capillary condensation within the PDMS-filled interstitial pores. We also show that the size of NPs has a crucial impact on the kinetics and extent of PDMS expulsion, illustrating the importance of capillary forces in inducing the PDMS expulsion. We demonstrate that the isolated polymer can be collected and reused to produce a new nanocomposite film. Our work provides insightful guidelines on how to design and fabricate end-of-life recyclable high-performance nanocomposites.

1. Introduction

Polymer nanocomposite films and membranes with extremely high loadings of nanoparticles (NPs) above ~ 50 vol % are highly desirable for a range of applications including protective coatings,[1–5] separation membranes,[6,7] optical films,[8,9] displays,[10] sensors[11,12] and energy devices[13,14] due to their exceptional mechanical and transport properties. Natural nanocomposites, such as nacre and tooth enamel, are known for their ultrahigh toughness and strength, which are achieved through high concentrations of hard NPs as well as the intricate nano/micro-scale structure of these composites.[1–5] Recent research has shown that it is possible to emulate the structure of these natural composites, resulting in nanocomposite films with high strength and toughness ideal for protective and structural applications.[1–5,15–18] Highly loaded nanocomposite films also exhibit excellent thermal and electrical conductivities due to the percolation of NPs, when thermally and electrically conductive NPs are used.[19–22] Various strategies have been developed to produce highly loaded nanocomposite films, coatings, and membranes, such as layer-by-layer processes,[3,4] polymerizing monomers in the interstitial pores of pre-assembled NP packings,[13,20,22,23] inducing infiltration of polymers into the voids of NP packings by capillary rise infiltration (CaRI)[9,16–20,24–26] or solvent-driven infiltration of polymer (SIP).[19,27]

To enable widespread utilization of these nanocomposites with extremely high loadings of NPs, it will become increasingly important to develop strategies for recycling these composites, which inevitably will require the separation and reclamation of NPs and polymers. Currently very few methods of efficiently separating NPs and polymers in nanocomposites without using high energy methods and harsh organic solvents exist.[28,29] Because of the challenges associated with separating polymers and NPs, nanocomposite wastes typically end up in landfills or are incinerated which leads to NPs entering the waste streams and potentially posing environmental hazards.[30–32] Designing and fabricating end-of-life recyclable nanocomposites will become increasingly important. Besides working towards a sustainable use of highly loaded nanocomposites, separating and removing unwanted polymeric contaminants from porous materials like NP packings is critical in maintaining the functionality and performance of the NP assemblies, which themselves have useful functionality.

In this study, we demonstrate that polymers can be spontaneously separated and recovered from nanocomposite films with high loadings of NPs with the aid of water from the vapor or the liquid phases. We use polydimethylsiloxane (PDMS)-infiltrated SiO_2 NP films as a model system because of the low glass transition temperature of PDMS and the high

concentration of SiO_2 in the nanocomposite (~ 64 vol %). The separation of PDMS from disordered SiO_2 NP packings depends strongly on the charge state of the SiO_2 NPs. Under high humidity and water, PDMS stays within the interstitial voids of ionized SiO_2 NP packings, whereas PDMS is expelled from the packings of unionized SiO_2 NPs by infiltrated water. We rationalize such dependence on the SiO_2 NP surface chemistry based on the kinetics of nucleation for capillary condensation.[33–35] The expulsion of PDMS is also strongly influenced by the relative humidity (RH) as well as the size of NPs, showcasing the role of capillarity in inducing polymer expulsion. The polymer expelled from the nanocomposite can be collected using an elastomer and reused for fabrication of nanocomposites. The method described in this study to induce separation of polymers and NPs from highly loaded nanocomposite films does not require any organic solvents and can be performed without relying on a highly energy-intensive process. The ability to separate and recover polymers from packings of NPs also has deep implications for the decontamination of porous membranes, soil and earth.

2. Results and Discussion

We use polymer-infiltrated NP films (PINFs) to test our hypothesis that water can induce separation of polymer and NPs in highly loaded nanocomposites. PINFs have emerged as a versatile class of nanocomposites with exceptional mechanical and transport properties owing to the high concentrations of NPs (> 64 vol%), large polymer-NP interfacial area and extreme nanoconfinement of polymers.[9,16–20,24–27] PINFs for this study are prepared by infiltrating a hydrophobic polymer, PDMS into the interstices of dense disordered packings of hydrophilic SiO_2 NPs. PDMS has a low glass transition temperature (< -100 °C),[36] thus its fate can be observed at room temperature. When a PDMS solution is spin coated onto a SiO_2 NP film, a bilayer film consisting of a PDMS overlayer and a SiO_2 NP packing partially filled with PDMS is initially formed; this bilayer film then spontaneously evolves into a PDMS-infiltrated SiO_2 NP film as the PDMS layer atop the SiO_2 NP packing infiltrates into the interstitial voids of the NP packing via capillary rise infiltration (CaRI);[9,16–20,24–26] when the void volume of the NP packing and the volume of dry PDMS are the same, a PINF with no residual PDMS overlayer is prepared. We fabricate such PINFs with thicknesses of ~ 250 nm (Figure S1) to study the fate of PDMS under high humidity or liquid water. The specifications of the SiO_2 NP aqueous dispersions used to prepare the SiO_2 NP films are given in **Table 1**. The refractive index of a bare SiO_2 NP film at the wavelength of 632.8 nm is 1.302. The refractive index of the film increases to 1.437 upon the infiltration of PDMS into the NP

interstitial voids, and its color changes as shown in **Figure 1**a. This refractive index value is slightly smaller than the theoretically estimated value based on the sum of the refractive indices per volume of the constituents (1.440), likely because a small volume of water exists within the film due to capillary condensation (< 10 vol %).[8,26,27]

Table 1. Specifications of the SiO_2 NP aqueous dispersions.[a)]

Name	Size [nm]	Concentration [wt %]	Counterion	pH
SM-30	7	30	Na+	10.0
TM-50	22	50	Na+	9.0
ST-YL	60	40	Na+	9.0-10.0

[a)]All are provided by the vendors.

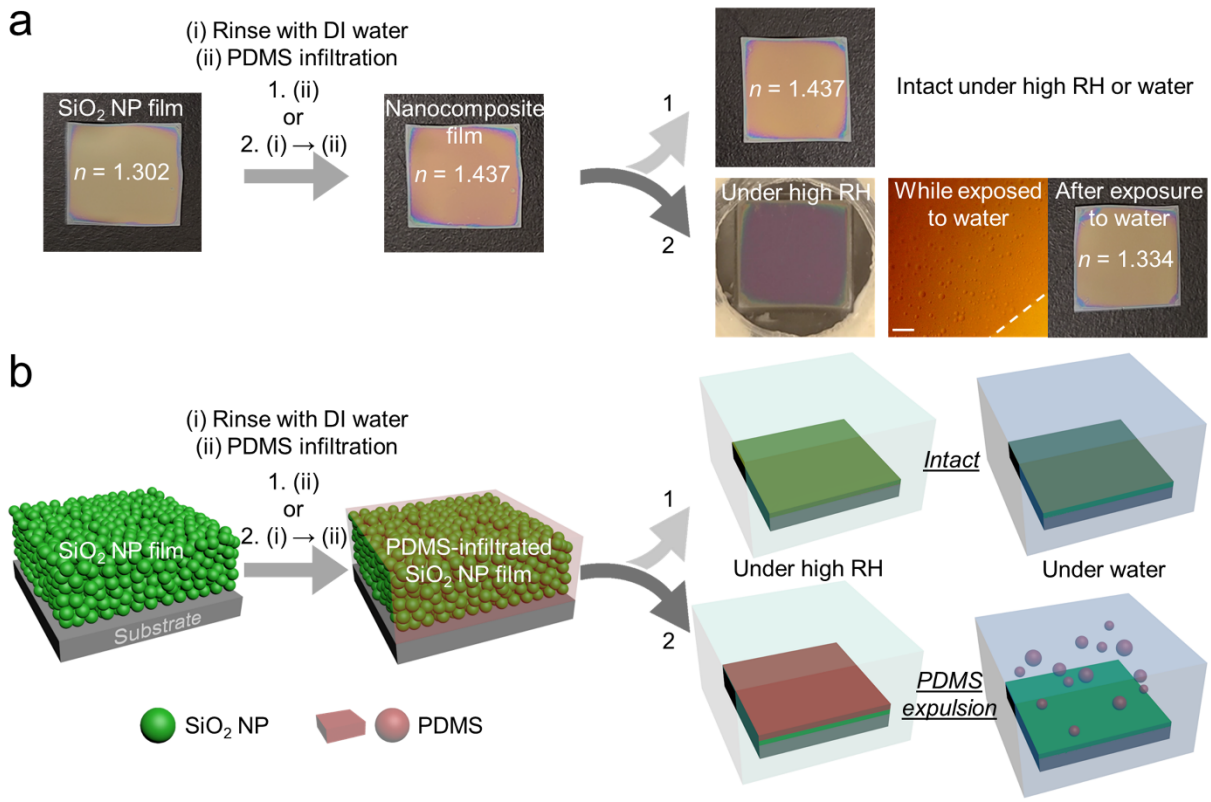

Figure 1. a) Actual appearance of the representative PDMS-infiltrated 22 nm-SiO_2 NP films under high humidity or liquid water depending on whether the base SiO_2 NP films are rinsed with DI water, and b) their schematic illustrations. *n* indicates refractive index of a film at the wavelength of 632.8 nm. The area above the white dashed line indicates where a water sessile drop is placed. The scale bar is 100 μm.

When an as-prepared PDMS-infiltrated 22 nm-SiO_2 NP film is exposed to high humidity (RH ~ 95%) or liquid water, no apparent changes in the macroscopic appearance of the film are observed, and the refractive index of the film, as determined by ellipsometry, remains constant. Serendipitously, we find that if PDMS is infiltrated into a SiO_2 NP film after the film was rinsed with deionized (DI) water and subsequently this PDMS-infiltrated SiO_2 NP film is exposed to high humidity, the color of the film changes dramatically from orange to purple as shown in Figure 1a. We focus on the analysis of these films that are prepared by rinsing the SiO_2 NP film with DI water prior to PDMS infiltration. When such a PINF is submerged in liquid water for 10 sec and then taken out, the refractive index of the film decreases to 1.334, indicating approximately 85% of PDMS has been removed. By placing a water sessile drop on top of the PINF and observing this area under a microscope (Figure S2), PDMS droplets are seen to emerge and rise from the surface (Figure 1a). After the expulsion of PDMS, the color of the area where the water sessile drop was placed returns to that of the bare SiO_2 NP films (Figure 1a), as seen in Figure S2. We also observe that PDMS is expelled from SiO_2 NP packings under the high humidity condition, if the packings are prepared using SiO_2 NP dispersions that were dialyzed against DI water. Likewise, when PDMS is infiltrated into a SiO_2 NP packing that was rinsed with DI water and then rinsed again with NaOH solution (pH 10), exposure of such a film does not induce any change in the appearance of the film under the high humidity condition.

The color change exhibited by the PINF upon the exposure to high humidity as shown in Figure 1a likely indicates a major change in the structure of the film. To gain a better insight into the structural change, spectroscopic ellipsometry is carried out using a two-layer Cauchy model; attempts to use other types of multi-layer Cauchy model leads to poor modeling. As presented in **Figure 2**b, a new layer with refractive index equal to that of PDMS is indeed formed on top as soon as the film is exposed to high humidity. At the same time, the refractive index of the NP layer (the underlayer) decreases, implying a loss of PDMS. However, the refractive index of the NP layer suggests the presence of water in the interstitial voids (~ 50 vol % of the voids). All these changes indicate that a bilayer consisting of a pure PDMS layer atop the NP layer is formed due to the expulsion of PDMS from the NP layer.

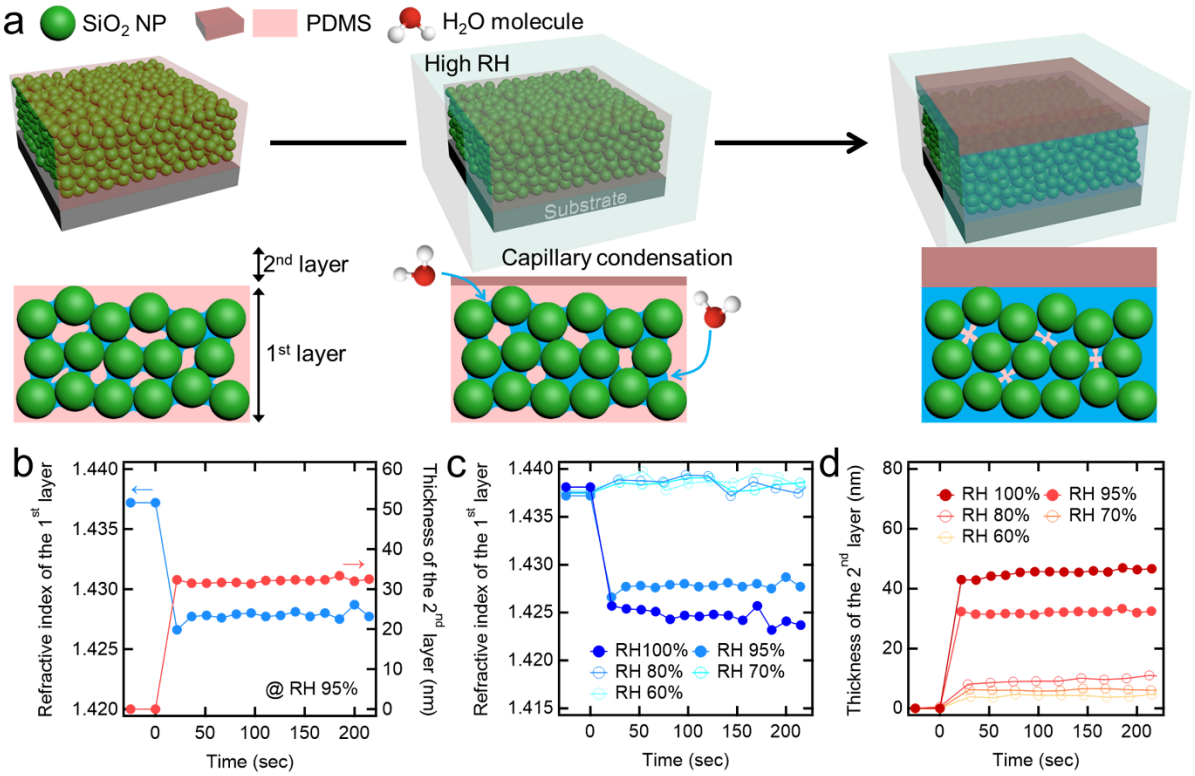

Figure 2. a) Schematic illustration of the mechanism by which PDMS is expelled from a PDMS-infiltrated SiO_2 NP film prepared from a DI water-rinsed SiO_2 NP film under high humidity, and b – d) actual changes in the refractive index of the NP underlayer (1st layer) and the thickness of the expelled PDMS layer (2nd layer) according to the PDMS expulsion from the PDMS-infiltrated 22 nm-SiO_2 NP film prepared from a DI water-rinsed SiO_2 NP film under various humidity conditions. The humidity starts to rise at time = 0 sec and reaches the target RH before the first data point is taken.

We believe that the driving force for the PDMS expulsion under high humidity is capillary condensation of water vapor within the NP interstitial voids of the NP packing. Typically, capillary condensation occurs when the interface between the condensate liquid-vapor phase can be stabilized at vapor pressure below the saturation pressure of the molecule due to the high negative curvature of the interface.[8,26,27] Analogous to capillary condensation, we believe that water vapor is undergoing capillary condensation in the PDMS-filled NP packing. Because the SiO_2 surface favors water over PDMS (Figure S4)[37] and PDMS has a high water permeability,[38,39] water is able to undergo capillary condensation and displace PDMS from the NP packing as depicted in Figure 2a. We believe that the nucleation of capillary bridges occurs at the contacts between SiO_2 NPs and the growth of these bridges push the PDMS out of the pores. As water vapor does under high humidity, water from the

bulk phase can permeate through the PDMS to induce nucleation and growth of capillary bridges in the interstitial voids of the PDMS-filled NP packing because of the high affinity of the SiO_2 NP surface for water over PDMS (Figure S4).[37] We do not believe the PDMS is displaced by water due gravitational or buoyancy-driven mechanisms since the Bond number (*Bo*) of the system, which represents the ratio of the gravitational force to interfacial tension force,[40] is far below 1 due to the nanoscale interstitial voids. However, we cannot completely rule out the possibility of the capillarity-induced wicking of water into the PDMS-filled pores displacing PDMS akin to wicking of water into air-filled pores.[41–43] We also confirm that PDMS introduced into the nanopores of the NP packing without using solvent[26] also undergoes expulsion from the nanopores upon exposure to high humidity or water, indicating that this behavior does not depend on the presence of residual solvent.

The thickness of the expelled PDMS layer and the refractive index of the NP underlayer reaches approximately 30 nm and 1.428, respectively. The amount of PDMS that is expelled from the NP packing is consistent with the amount expected from the refractive index reduction in the NP underlayer, which now consists of water, SiO_2 NPs and residual PDMS. The reduction in the refractive index of the NP underlayer and the increase in the thickness of the expelled PDMS layer increase with RH, as shown in Figure 2c and d. These results support that the expulsion of PDMS is driven by the capillary condensation of water vapor in the PDMS-filled NP packing.

We now turn our attention back to the two different types of SiO_2 NP films that showed vastly different behavior when exposed to the high humidity or liquid water. The tendency of polymer to undergo expulsion depends on whether the bare SiO_2 NP film is rinsed with DI water or not before the PDMS infiltration; such difference points to the fact that the interactions between PDMS and the SiO_2 NP surface is altered due to the charge state of the SiO_2 NP surface. Since the isoelectric point of SiO_2 surfaces is around 3,[44] SiO_2 NPs are negatively charged and the charge is balanced by cationic counterions (M^+s) in water at the solution pH of 9 – 10 (the condition used in this study). Prior studies have classified the surface of SiO_2 into three types: Q^2, Q^3, and Q^4 based on the areal density of SiOH groups; the surface of the NPs used in this study has been previously categorized as Q^3, possessing ~ 4.7 SiOH groups per nm^2.[45,46] About 20% of the SiOH groups on the surfaces of Q^3 are known to deprotonate and form SiO^--M^+ groups in water at the pH of 9 – 10.[46,47] The SiO_2 NP films prepared by spin coating the dispersions with Na^+ counterions, thus would have a large number of SiO^-Na^+ surface groups (**Figure 3**a). In contrast, when such a film is rinsed with DI water which has a pH of 5.5-6.0, a large number of the SiO^-Na^+ groups become

protonated to form SiOH groups (Figure 3a). This change in the surface chemistry is verified by characterizing the NP surface using energy-dispersive X-ray spectroscopy (EDS). As shown in Figure 3b, the peaks that represent O and Si remain identical in the two SiO_2 NP films, whereas the peak assigned to Na is only observed in the as-prepared unrinsed SiO_2 NP film (inset of Figure 3b). Similar changes in the surface chemistry are observed for the SiO_2 NP films with different NP sizes studied in this work, as seen in Figure S5a.

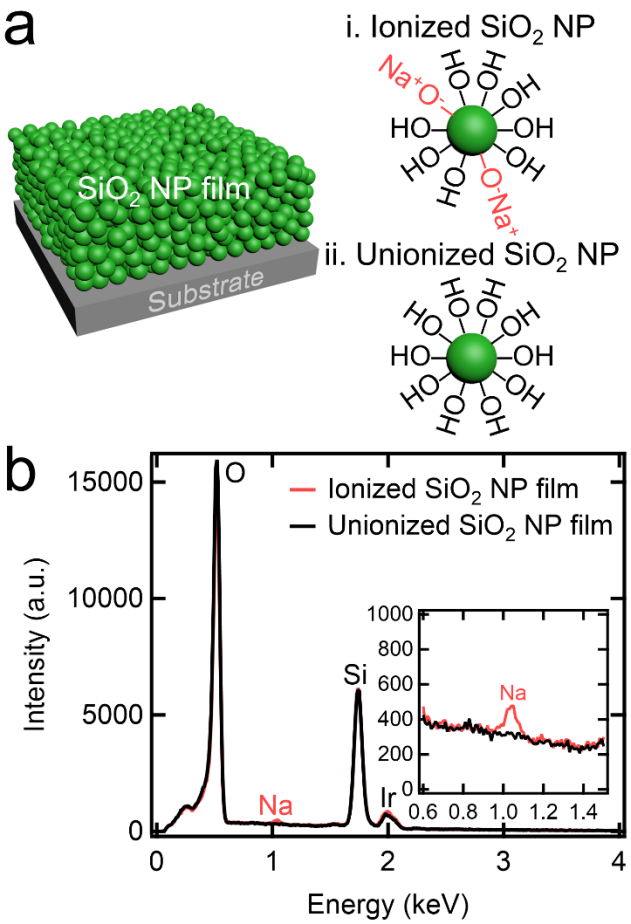

Figure 3. a) Schematic illustration of the ionized and unionized SiO_2 NP films, and b) element characterization of the representative 22 nm-SiO_2 NP films in the two cases using EDS analysis. The peak assigned to Ir is attributed to the metallic coating that is deposited prior to scanning electron microscope observation to prevent charging.

Interestingly, both the ionized and the unionized SiO_2 surfaces have preferential interactions with water over PDMS as determined by contact angle measurements (Figure S4). Thus, solely based on thermodynamic arguments, PDMS expulsion would be predicted for both cases. However, our experimental results unequivocally show that there is a drastic

difference between the two cases. To understand how the change in the surface chemistry of SiO_2 NPs can induce the expulsion of PDMS under high humidity and liquid water, we rely on the kinetics of capillary condensation in solid mesopores filled with liquid media. In our system, the SiO_2 NP surfaces and PDMS constitute the solid and liquid phases, respectively. There exists a critical free energy barrier to induce the nucleation and growth of capillary bridges in nanoscale pores.[33–35] When we estimate the critical free energy barriers for both ionized and unionized 22 nm-SiO_2 NP packings (see Supporting Information for details), the estimated critical free energy barrier for the ionized SiO_2 NP packing is greater by at least ~ 30 k_BT (where k_B is the Boltzmann constant and T is temperature) compared to the unionized SiO_2 NP packing. Based on these estimations, we believe that water vapor cannot nucleate in the interstitial pores of the ionized SiO_2 NP packing due to the larger critical free energy barrier, whereas water vapor can nucleate and grow as condensed liquid water in the unionized NP interstitial pores, resulting in the massive expulsion of PDMS. Likewise, liquid water likely experiences a similar energy barrier to nucleate capillary bridges for the ionized SiO_2 NP packing, and thus aqueous bridges are not able to growth and thus PDMS remain intact within the interstitial voids.

The driving force for capillary condensation increases as the NP size decreases due to the increased curvature of the interface.[8,26,27] Consistent with this, the increase in the thickness of the expelled PDMS layer and the reduction in the refractive index of the NP underlayer under high RH are greater with decreasing NP size at a fixed RH, as presented in **Figure 4**a. Moreover, the rate at which PDMS is expelled from the NP packing due to capillary condensation of water vapor becomes faster with decreasing NP size, as shown in Figure 4b, indicating the importance of thermodynamic driving force. Consistent with these observations, when PDMS-infiltrated SiO_2 NP films are submerged under water, as the NP size decreases, a larger volume of water infiltrates, expelling a larger volume of PDMS as shown in Figure 4c. The fraction of PDMS expelled as a function of RH increases with decreasing NP size, as summarized in Figure 4c, indicating that smaller NP size and higher RH are key features that induces PDMS expulsion due to water infiltration.

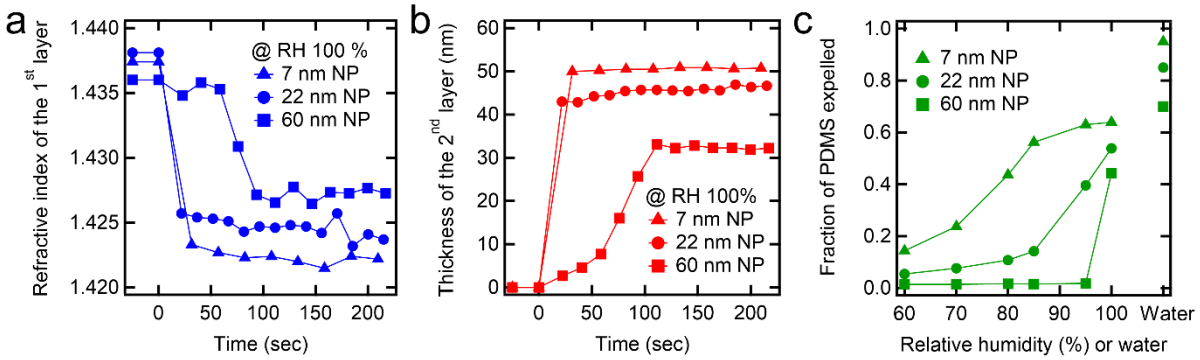

Figure 4. NP size effects on the PDMS expulsion from the PDMS-infiltrated SiO_2 NP films prepared from DI water-rinsed SiO_2 NP films. a) The changes in the refractive index of the SiO_2 NP underlayer (1st layer) at RH 100 %. b) The changes in the thickness of the expelled PDMS layer (2nd layer) at RH 100 %. c) The changes in the fraction of the PDMS expelled under various humidity conditions and exposure to liquid water.

One of the essential steps that must be implemented to enable the recycling of the separated polymer is its collection. PDMS expelled from the nanocomposite under water can be directly collected using various methods.[48,49] and reused. In contrast, the expelled PDMS layer under high humidity does not spontaneously detach from the NP packing. One way to collect the expelled PDMS under high humidity is to exploit elastomer that functions as a collection reservoir. A crosslinked PDMS elastomer slab is placed on top of a PDMS-infiltrated SiO_2 NP (unionized) film and is exposed to high RH; the expelled PDMS is absorbed into the elastomer and freed from the NP packing by detaching the elastomer, as shown in **Figure 5**a. In case of using a PDMS-infiltrated 7 nm-SiO_2 NP film, the refractive index of the film decreases from 1.437 to ~ 1.36 at RH ~ 100% (Figure 5a), indicating approximately 60 % of PDMS has been recovered, consistent with the results in Figure 4c. The PDMS collected in the elastomer can be reused in various ways; for example, when this PDMS-loaded elastomer is placed on top of another SiO_2 NP film, the mobile PDMS chains infiltrate into the interstitial voids,[26] resulting in the formation of a new PINF, as evidenced by the increase of the refractive index of the film from 1.302 to ~ 1.44 (Figure 5a).

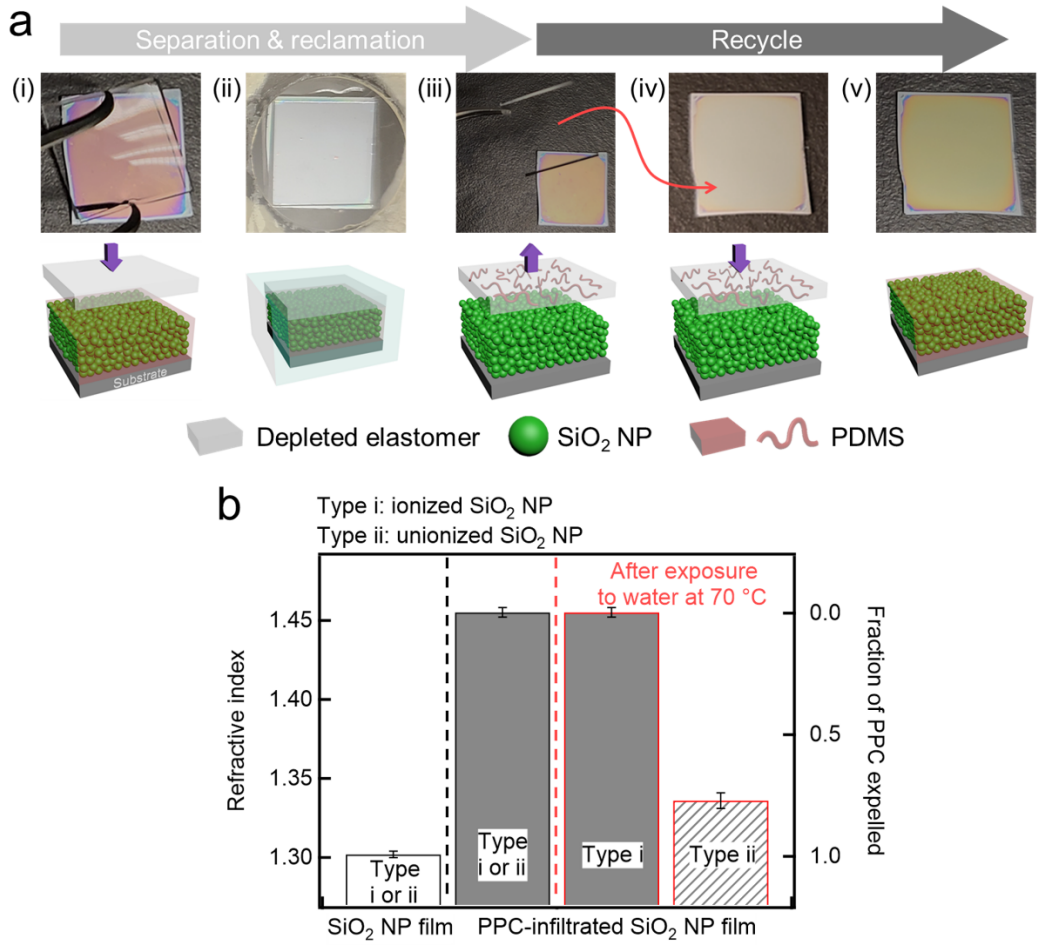

Figure 5. a) Photographic images and schematic illustration of the collection and reuse of the PDMS separated from the PDMS-infiltrated 7 nm-SiO_2 NP (unionized) films under high humidity (RH ~ 100%). (i) A crosslinked PDMS elastomer slab is placed atop the PINF; (ii) the PINF with the elastomer slab on top is exposed to 100% RH; (iii) the elastomer slab carrying the expelled PDMS is removed from the PINF; (iv) the elastomer slab is placed on top of a newly prepared NP film; (v) PDMS from the elastomer slab is infiltrated into the interstices of the NP film and a new PINF is prepared. b) Changes in the refractive index of the PPC-infiltrated 22 nm-SiO_2 NP films prepared from ionized and unionized SiO_2 NP films before and after exposure to heated water. For another SiO_2 NP film, 7 nm-unionized SiO_2 NP film with a thickness of ~ 200 nm is used. PPC is expelled only from the PPC-infiltrated SiO_2 NP film prepared from the unionized SiO_2 NP film under the heated water.

To demonstrate that the separation of polymer is not limited to a low glass transition temperature polymer such as PDMS and that high glass transition temperature thermoplastics that are used for nanocomposite fabrication can be recovered using the same approach, we test

the feasibility of separating polypropylene carbonate (PPC, refractive index = 1.460) which has a glass transition temperature of 35 °C[50] from SiO_2 NP packings. The refractive index of a PPC-infiltrated SiO_2 NP film is 1.454, as shown in Figure 5b. The film is placed in a vial filled with DI water and heated in a water bath at 70 °C for 10 min. The refractive index of the PPC-filled ionized SiO_2 NP packing remains constant, whereas that of the PPC-filled unionized SiO_2 NP packing decreases to 1.336 (Figure 5b), indicating approximately 80% removal of PPC. This extent of expulsion is consistent with the case with PDMS.

3. Conclusion

In this work, we have demonstrated that polymers can be spontaneously separated from PINFs via capillary condensation of water into the interstices of NP packings under high humidity or exposure to liquid water. The separation of PDMS depends strongly on the energy barrier to induce the nucleation and growth of capillary condensation in SiO_2 NP packings which depends on the charge state of NPs as well as the RH and the NP size. The results of this study have implications on the reclamation of non-crosslinked thermoplastic polymers from nanocomposites for recycling as well as decontamination of porous materials such as NP packings. Moreover, the study provides guidelines on designing end-of-life recyclable nanocomposites with high loadings of NPs. There are several open questions that warrant future studies. The type of counterion, for example, could change the interaction of ionized SiO_2 NP surfaces with water[51] and in turn affect the extent of polymer expulsion from NP packings. The impact of the NP distribution and the structure of NP packings on the separation of polymer and NPs requires more detailed future investigation. Moreover, the mechanism by which capillary bridges nucleate and grow will benefit substantially from the development of theoretical and computational approaches that account for water density fluctuations in the complex topology of NP packings.[52]

4. Experimental Section/Methods

Materials: Monodisperse PDMS (M_n = 15k g mol^{-1}, P7273-DMS) and UV-curable PDMS (KER-4690 A and B) are purchased from Polymer Source (Dorval, QC, Canada) and Shin-Etsu Chemical Co., Ltd (Tokyo, Japan), respectively. PPC (M_n ~ 50k g mol^{-1}, 389021) is purchased from MilliporeSigma (St. Louis, MO, USA). For the SiO_2 NP aqueous dispersions with different NP sizes, Ludox® SM-30 and TM-50 are obtained from MilliporeSigma, and Snowtex® ST-YL is generously provided by Nissan Chemical America Corp. (Houston, TX, USA). The specifications of the SiO_2 NP aqueous dispersions are given in **Table 1**. Isopropyl

alcohol (Certified ACS Plus), NaOH solution (1 N/Certified), toluene (HPLC Grade), and chloroform (HPLC Grade) are purchased from Fisher Scientific Co LLC (Pittsburgh, PA, USA). Ethanol (200 Proof) is obtained from Decon Laboratories Inc (King of Prussia, PA, USA).

Preparation of bare SiO_2 NP films and PINFs: As substrates, Si wafers (452, UniversityWafer, Inc., South Boston, MA, USA) are cleaved into approximately 1.5 × 1.5 cm^2 pieces, and the surface of the cleaved wafers are rinsed with isopropyl alcohol and DI water (18.2 MΩ·cm), followed by 5 min of oxygen plasma (PDC-32G, Harrick Plasma Inc., Ithaca, NY, USA) treatment to remove residual organic contaminants. The stock SiO_2 NP aqueous dispersions are diluted with DI water to ~ 15 wt %. Some of the diluted dispersions are dialyzed for 120 hr against DI water, which is replaced every 24 hr, using dialysis tubes (10k MWCO, 68100, Fisher Scientific Co LLC). Prior to use, all the diluted dispersions are sonicated for at least 2 hr to ensure homogeneous dispersion of SiO_2 NPs, and then filtered using hydrophilic syringe filters with a size cut-off of 0.45 μm (09-720-005, Fisher Scientific Co LLC) to remove NP aggregates. SiO_2 NP films with thicknesses of ~ 250 nm are prepared on the Si substrates by spin coating the filtered dispersion using a spin coater (WS-400BZ-6NPP/Lite, Laurell Technologies Corporation, North Wales, PA, USA) at 2500 – 3000 rpm for 1.5 min. Some of the SiO_2 NP films are rinsed with DI water or NaOH solution (pH 10) for 10 sec to deionize or re-ionize the NP surfaces, respectively.

PDMS (monodisperse PDMS or 1:1 mixture of the UV-curable PDMS precursors A and B) and PPC are dissolved in toluene and chloroform at a concentration of 4 wt %, respectively. Polymer layers of the desired thicknesses are coated on top of the SiO_2 NP films by spin coating the polymer solutions at 4000 – 5000 rpm for 30 sec. PDMS infiltrates into the interstices of the SiO_2 NPs via CaRI during/after spin coating, forming PDMS-infiltrated SiO_2 NP films. Unless otherwise noted, the monodisperse PDMS is used in this study. The UV-curable PDMS-infiltrated SiO_2 NP film is exposed to UV (illuminance ~ 100 mW/cm^2, wavelength = 365 nm) for 30 sec and aged for 24 hr, to fully cure the PDMS. This film is used to obtain a SEM image of a PDMS-infiltrated SiO_2 NP film (Figure S1) rather than to demonstrate the separation of polymer because uncured PDMS may contaminate the SEM chamber under vacuum. The bilayer film consisting of the PPC layer atop the SiO_2 NP film is heated in an oven (Model 20 Lab Oven, Quincy Lab, Inc., South Beloit, IL, USA) at 80 °C for 3 hr to induce infiltration of PPC into the interstices of the NP packing via CaRI.

Film characterization: The surface chemistry of the SiO_2 NP films is characterized by EDS analysis using an EDS detector (EDAX, AMETEK, Inc., Berwyn, PA, USA) mounted

on a scanning electron microscope (SEM) (Quanta 600 FEG ESEM, FEI Company, Hillsboro, OR, USA). Prior to analysis, the films are coated with 4 nm Ir layers using a sputter coater (Q150TES, Quorum Technologies Ltd., Lewes, UK) to prevent possible charging. After focusing the films at a 5 kV electron beam voltage in the SEM, EDS signals are detected for 1 min. The analysis is performed using the TEAM™ EDS Analysis System (EDAX, Mahwah, NJ, USA). The microstructure of the UV-cured PDMS-infiltrated SiO_2 NP film is captured using a high-resolution SEM (JSM-7500F, JEOL Ltd., Tokyo, Japan) under conditions of 5 kV electron beam voltage and 20 μA emission current. The film is coated with a 4 nm Ir layer prior to analysis as well.

The thickness and refractive index of films are determined using a spectroscopic ellipsometer (SE-2000, Semilab, Budapest, Hungary). The ellipsometer measures the amplitude ratio (Ψ) and the phase difference (Δ) of the complex reflection coefficients of light polarized parallel and perpendicular to the plane of incidence. The measurements are carried out at 75 ° of incidence angle in the photon energy range of 1.3 – 4.5 eV, and the measured optical data are analyzed by the SEA software to extract the thicknesses and refractive indices. Each transparent layer is modelled as a Cauchy layer, and the refractive index is represented by $n = A + B/\lambda^2 + C/\lambda^4$, where A, B, and C are optical constants and λ is wavelength of light. Modelling is performed with a small mean square error (< 5). The RH of the air surrounding the films is controlled using a humidity chamber (operated by a mass flow controller to ensure the ratio of dry and wet air inlet) compatible with the ellipsometer. For measurements in increased RH environments, the initial spectra are recorded at 40% RH, which is followed by an increase to a set RH value which is then kept constant in time.

Environmental ellipsometric porosimetry is carried out in the same humidity chamber by recording ellipsometric spectra stepwise at increasing/decreasing RH (in the RH range between 2%–100%-2%). Lorentz-Lorenz effective medium approximation (EMA) is used to model the refractive index of the SiO_2 NP packings partially filled with air and adsorptive (water) molecules to obtain the volume adsorbed/desorbed isotherms from the fitted refractive index values.[53] Porosity is calculated using the Lorentz-Lorenz EMA for the water filled SiO_2 NP packings at RH = 100%, and the pore size distribution is obtained via the modified Kelvin-equation.[53,54]

An upright optical microscope (Euromex, Arnhem, Netherlands) mounted with a CCD camera (MU800, AmScope, Irvine, CA, USA) is used in the reflection mode to observe microscopic changes in the PDMS-infiltrated SiO_2 NP films under water. A 5 uL water drop is placed onto the film using a micropipette (0.5 – 10 uL, Eppendorf, Hamburg, Germany),

and images are taken the rim of the water drop to highlight the difference between the presence and absence of water. Contact angles are determined using a goniometer (Attension, Biolin Scientific, Gothenburg, Sweden).

Collection and reuse of the expelled PDMS under high RH using depleted elastomers: The 1:1 mixture of the UV-curable PDMS precursors A and B is degassed using a vacuum degasser. The mixture is then poured onto a Petri dish and exposed to UV (illuminance ~ 100 mW/cm^2, wavelength = 365 nm) for 30 sec and aged for 24 hr, to fully cure the PDMS. The cured elastomer is cleaved into approximately 1.5 × 1.5 cm^2 pieces and left in a toluene bath for 5 days, replacing the toluene used daily. Uncrosslinked chains are leached out using toluene, resulting in a depleted elastomer.[55] The depleted elastomers are stored in ethanol for 24 hr, followed by 24 hr in DI water to remove residual solvents. The PDMS-infiltrated SiO_2 NP (unionized) film, on which the depleted elastomer is in contact, is exposed to high humidity (RH ~ 100%) for 10 min, and the expelled PDMS is collected into the elastomer. After repeating the collection from 3 different films, the PDMS loaded in the elastomer can be reused to fabricate a new PDMS-infiltrated SiO_2 NP film by contacting the elastomer with a new SiO_2 NP film for 1 min at RH ~ 10% via leaching-enabled CaRI; the mobile PDMS chains infiltrate into the interstitial voids.[26]

Supporting Information

Supporting Information is available from the Wiley Online Library or from the author.

Acknowledgements

This work was supported by Penn MRSEC (DMR 1720530). M.F. acknowledges support by an UCL Chemical Engineering Impact PhD studentship sponsored by Semilab.

Received: ((will be filled in by the editorial staff))
Revised: ((will be filled in by the editorial staff))
Published online: ((will be filled in by the editorial staff))

References

[1] A. Sellinger, P. M. Weiss, A. Nguyen, Y. Lu, R. A. Assink, W. Gong, C. J. Brinker, *Nature* **1998**, *394*, 256.

[2] E. Munch, M. E. Lanuney, D. H. Alsem, E. Saiz, A. P. Tomsia, R. O. Ritchie, *Science* **2008**, *322*, 1516.

[3] L. J. Bonderer, A. R. Studart, L. J. Gauckler, *Science* **2008**, *319*, 1069.

[4] B. Yeom, T. Sain, N. Lacevic, D. Bukharina, S. H. Cha, A. M. Waas, E. M. Arruda, N. A. Kotov, *Nature* **2017**, *543*, 95.

[5] H. Zhao, S. Liu, Y. Wei, Y. Yue, M. Gao, Y. Li, X. Zeng, X. Deng, N. A. Kotov, L. Guo, L. Jiang, *Science* **2022**, *375*, 551.

[6] Y. Deng, J. Chen, C. Chang, K. Liao, K. Tung, W. E. Price, Y. Yamauchi, K. C. -W. Wu, *Angew. Chem. Int. Ed.* **2016**, *128*, 12985.

[7] F. Ding, J. Liu, S. Zeng, Y. Xia, K. M. Wells, M.-P. Nieh, L. Sun, *Sci. Adv.* **2017**, *3*, e1701212.

[8] Z. Gemici, P. I. Schwachulla, E. H. Williamson, M. F. Rubner, R. E. Cohen, *Nano Lett.* **2009**, *9*, 1064.

[9] B. Q. Kim, Y. Qiang, K. T. Turner, S. Q. Choi, D. Lee, *Adv. Mater. Interfaces* **2021**, *8*, 2001421.

[10] C. Dang, J. Lee, C. Breen, J. S. Steckel, S. Coe-Sullivan, A. Nurmikko, *Nat. Nanotechnol.* **2012**, *7*, 335.

[11] J. Lee, S. Kim, J. Lee, D. Yang, B. C. Park, S. Ryu, I. Park, *Nanoscale* **2014**, *6*, 11932.

[12] A. S. Pawbake, R. G. Waykar, D. J. Late, S. R. Jadkar, *ACS Appl. Mater. Interfaces* **2016**, *8*, 3359.

[13] D. W. Wang, F. Li, J. Zhao, W. Ren, Z. G. Chen, J. Tan, Z. S. Wu, I. Gentle, G. Q. Lu, H. M. Cheng, *ACS Nano* **2009**, *3*, 1745.

[14] E. Bakangura, L. Wu, L. Ge, Z. Yang, T. Xu, *Prog. Polym. Sci.* **2016**, *57*, 103.

[15] Q. Chen, S. Gong, J. Moll, D. Zhao, S. K. Kumar, R. H. Colby, *ACS Macro Lett.* **2015**, *4*, 398.

[16] Y. Qiang, K. T. Turner, D. Lee, *Macromolecules* **2023**, *56*, 122.

[17] Y. Qiang, S. S. Pande, D. Lee, K. T. Turner, *ACS Nano* **2022**, *16*, 6372.

[18] Y. Jiang, J. L. Hor, D. Lee, K. T. Turner, *ACS Appl. Mater. Interfaces* **2018**, *10*, 44011.

[19] R. B. Venkatesh, N. Manohar, Y. Qiang, H. Wang, H. H. Tran, B. Q. Kim, A. Neuman, T. Ren, Z. Fakhraai, R. A. Riggleman, K. J. Stebe, K. Turner, D. Lee, *Annu. Rev. Chem. Biomol. Eng.* **2021**, *12*, 411.

[20] C. Harito, D. v. Bavykin, B. Yuliarto, H. K. Dipojono, F. C. Walsh, *Nanoscale* **2019**, *11*, 4653.

[21] H. Zhu, Y. Li, Z. Fang, J. Xu, F. Cao, J. Wan, C. Preston, B. Yang, L. Hu, *ACS Nano* **2014**, *8*, 3606.

[22] R. Hoffmann, V. Baric, H. Naatz, S. O. Schopf, L. Mädler, A. Hartwig, *ACS Appl. Nano Mater.* **2019**, *2*, 2273.

[23] H. Zhang, M. Popp, A. Hartwig, L. Mädler, *Nanoscale* **2012**, *4*, 2326.

[24] Y. R. Huang, Y. Jiang, J. L. Hor, R. Gupta, L. Zhang, K. J. Stebe, G. Feng, K. T. Turner, D. Lee, *Nanoscale* **2015**, *7*, 798.

[25] J. L. Hor, Y. Jiang, D. J. Ring, R. A. Riggleman, K. T. Turner, D. Lee, *ACS Nano* **2017**, *11*, 3229.

[26] R. B. Venkatesh, S. H. Han, D. Lee, *Nanoscale Horiz.* **2019**, *4*, 933.

[27] N. Manohar, K. J. Stebe, D. Lee, *ACS Macro Lett.* **2017**, *6*, 1104.

[28] M. Prinçaud, C. Aymonier, A. Loppinet-Serani, N. Perry, G. Sonnemann, *ACS Sustain. Chem. Eng.* **2014**, *2*, 1498.

[29] J. Jiang, G. Deng, X. Chen, X. Gao, Q. Guo, C. Xu, L. Zhou, *Compos. Sci. Technol.* **2017**, *151*, 243.

[30] J. M. Garcia, M. L. Robertson, *Science* **2017**, *358*, 870.

[31] Y. Yang, R. Boom, B. Irion, D. J. van Heerden, P. Kuiper, H. de Wit, *Chem. Eng. Process.* **2012**, *51*, 53.

[32] J. Pourchez, C. Chivas-Joly, C. Longuet, L. Leclerc, G. Sarry, J. M. Lopez-Cuesta, *Environ. Sci.: Nano* **2018**, *5*, 1951.

[33] F. Restagno, L. Bocquet, T. Biben, *Phys. Rev. Lett.* **2000**, *84*, 2433.

[34] T. Hiratsuka, H. Tanaka, M. T. Miyahara, *J. Chem. Phys.* **2016**, *144*, 164705.

[35] C. Desgranges, J. Delhommelle, *Langmuir* **2019**, *35*, 15401.

[36] K. Xing, S. Chatterjee, T. Saito, C. Gainaru, A. P. Sokolov, *Macromolecules* **2016**, *49*, 3138.

[37] B. P. Binks, J. H. Clint, *Langmuir* **2002**, *18*, 1270.

[38] G. C. Randall, P. S. Doyle, *Proc. Natl. Acad. Sci. U. S. A.* **2005**, *102*, 10813.

[39] P. Bian, Y. Wang, T. J. McCarthy, *Macromol. Rapid Commun.* **2021**, *42*, 2000682.

[40] N. J. Alvarez, L. M. Walker, S. L. Anna, *J. Colloid Interface Sci.* **2009**, *333*, 557.

[41] B. K. Primkulov, J. Y. Y. Chui, A. A. Pahlavan, C. W. Macminn, R. Juanes, *Phys. Rev. Lett.* **2020**, *125*, 174503.

[42] J. Andre, K. Okumura, *Langmuir* **2020**, *36*, 10952.

[43] O. McRae, T. S. Ramakrishnan, J. C. Bird, *J. Colloid Interface Sci.* **2022**, *608*, 1919.

[44] M. Kosmulski, *Chemical Properties of Material Surfaces*, Marcel Dekker, New York, **2001**.

[45] L. T. Zhuravlev, *Colloids Surf. A Physicochem. Eng. Asp.* **2000**, *173*, 1.

[46] F. S. Emami, V. Puddu, R. J. Berry, V. Varshney, S. V. Patwardhan, C. C. Perry, H. Heinz, *Chem. Mater.* **2014**, *26*, 2647.

[47] J. M. Rimsza, R. E. Jones, L. J. Criscenti, *J. Colloid Interface Sci.* **2018**, *516*, 128.

[48] R. K. Gupta, G. J. Dunderdale, M. W. England, A. Hozumi, *J. Mater. Chem. A* **2017**, *5*, 16025.

[49] J. Gu, L. Ji, P. Xiao, C. Zhang, J. Li, L. Yan, T. Chen, *ACS Appl. Mater. Interfaces* **2021**, *13*, 36679.

[50] Y. Qin, L. Chen, X. Wang, X. Zhao, F. Wang, *Carbohydr. Polym.* **2011**, *84*, 329.

[51] M. C. Gurau, S. M. Lim, E. T. Castellana, F. Albertorio, S. Kataoka, P. S. Cremer, *J. Am. Chem. Soc.* **2004**, *126*, 10522.

[52] S. Prakash, E. Xi, A. J. Patel, *Proc. Natl. Acad. Sci. U. S. A.* **2016**, *113*, 5508.

[53] A. Alvarez-Fernandez, B. Reid, M. J. Fornerod, A. Taylor, G. Divitini, S. Guldin, *ACS Appl. Mater. Interfaces* **2020**, *12*, 5195.

[54] M. R. Baklanov, K. P. Mogilnikov, V. G. Polovinkin, F. N. Dultsev, *J. Vacuum Science & Technology B: Microelectronics and Nanometer Structures* **2000**, *18*, 1385.

[55] R. B. Venkatesh, D. Lee, *Macromolecules* **2022**, *55*, 8659.

Polymers are spontaneously separated and recovered from high nanoparticle-content nanocomposite films with the aid of water from the vapor or liquid phases. The charge state of nanoparticles plays a significant role in the propensity of water to undergo capillary condensation within the polymer-filled interstitial pores. Our work provides insightful guidelines on how to design and fabricate end-of-life recyclable high-performance nanocomposites.

B. Q. Kim, M. Füredi, R. B. Venkatesh, S. Guldin, D. Lee*

Water-Induced Separation of Polymers from High Nanoparticle-Content Nanocomposite Films